# Redundant Upper Limb Exoskeleton Robot with Passive Compliance

J.M.P Gunasekara, R.A.R.C. Gopura
Dept. of Mechanical Engineering
University of Moratuwa
Katubedda, Sri Lanka
malingunasekara@gmail.com, gopura@ieee.org

T.S.S. Jayawardena
Dept. of Textile and Clothing Technology
University of Moratuwa
Katubedda, Sri Lanka
jaya@uom.lk

***Abstract* — Enhancing physical Human-Robot Interaction (pHRI) is an important design aspect in upper limb exoskeleton robots. The level of manipulation provided by an exoskeleton robot has a significant effect to perform daily tasks. This paper evaluate performance of a 6 degree of freedom (DoF) upper limb exoskeleton robot. The detailed mechanical design of the robot is presented with the novel features included in order to improve the pHRI. The exoskeleton robot consists of six DoF and two flexible bellow couplings are used to provide translational DoF at wrist and elbow joints. Moreover, flexible bellow couplings are positioned at specific locations in order to enhance the kinematic redundancy. The benefit of compliance due to the flexible bellow coupling at wrist joint of the robot is verified with reference to manipulability variation of the kinematic model of human lower arm.**

**Keywords: compliance, exoskeleton, redundancy, manipulability**

## I. INTRODUCTION

An exoskeleton robot is a special kind of robot compared to industrial robots, since human-robot interaction is utmost significant during operation. Typically, exoskeleton robots are used in different applications such as human power amplification, motion assist, rehabilitation, haptic interface in virtual reality [1]. It is clear that there exists a close interaction with the wearer in all above cases. In general, exoskeleton robots have two types of interactions with wearer: physical human-robot interaction (pHRI) and cognitive human-robot interaction (cHRI) [2]. In pHRI, suitability of a robot to the wearer is investigated in terms of safety, comfort, degree of manipulation, workspace, weight, singularity and ease of use [2]. Controlling aspects of a robot are considered under cHRI all over the time.

Since the human upper limb is anatomically complex, providing comfort to wearer is a challenging design aspect in exoskeleton robots. Joint axes misalignment between human joint and robot joint is one of the roots to produce the discomfort to wearer. This causes to generate reactive forces and torques at connecting points between exoskeleton robot and the wearer. However, obtaining the correct alignment between robot joint axis and human joint axis is practically difficult due to soft tissue deformations, variations of inter- and intra-subject anatomical features, etc. Furthermore, addressing issues relating to restore the comfort is basically coming under kinematic of exoskeleton rather than control aspect [3]. Different methodologies are considered to improve comfort to wearer. This includes, increase of number of degree of freedom (DoF) in kinematic chain, use of passive mechanisms and adding the compliance. Recent exoskeleton robots have a trend to use passive DoF in its kinematic chain to minimize kinematic discrepancies causes due to joint axis misalignments [4]. Introducing passive compliance is an another approach to minimize the axes misalignment [5]. In most cases, the passive compliance is added to the exoskeleton through a mechanism rather than as a joint. In particular, the added mechanisms tend to increase the complexity of exoskeleton structure and it does not alter the kinematic performance of robot. Therefore, introduced passive compliance may not improve dexterity performances, since such compliances may not change the number of DoF in a kinematic chain.

Typically, human upper limb consists of 7 DoF, mainly distributed along shoulder, elbow and wrist [6]. However, displacement of instantaneous centre of rotation (ICR) at shoulder joint may cause to increase the DoF in human upper limb [3]. Several models are proposed for the human upper limb in the literature taking the complexity into account and those kinematic models use more than 7 DoF [3][7][8]. Despite the higher DoF in human kinematic model, many upper limb exoskeleton robots have been used the same DoF available in human upper limb. Typically, full upper limb exoskeleton robots have used 7 DoF [9][10]. Moreover, it can be seen that 4 DoF kinematic model is proposed for human lower arm. In general, if DoF associated with robot is higher than that of human limb, it may cause to introduce kinematic redundancy and further, it helps to reduce the kinematic discrepancies generated due to axes misalignment [3]. Therefore, providing more DoF in exoskeleton robot is an interesting direction to improve comfort to wearer.

This paper proposes a mechanical design and a performance evaluation for the 6 DoF upper limb exoskeleton robot for the motion assist considering effect of kinematic redundancy with passive compliance. The proposed robot supports elbow flexion-extension, forearm supination-pronation, wrist flexion-extension and wrist ulnar–radial deviation. Flexible bellow couplings are attached to kinematic chain of the exoskeleton robot at wrist and elbow joint in order to enhance kinematic

978-1-4799-4598-6/14/$31.00 ©2014 IEEE

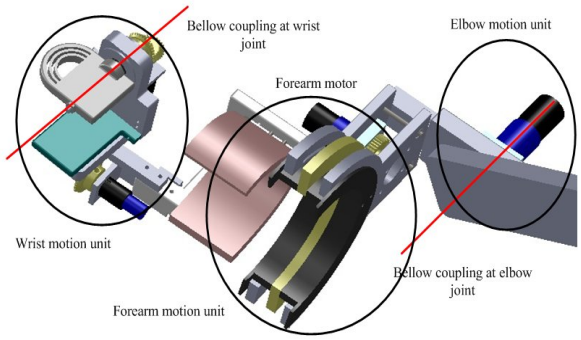


Figure. 1. The 6-DoF exoskeleton with main motion units

redundancy. In particular, the bellow coupling provides two DoF in translational direction which results more DoF than that are available in human lower arm. Furthermore, the compliance is introduced at elbow and wrist using the flexible bellow coupling. The degree of manipulation of exoskeleton robot is compared with kinematic model of the human lower arm and significance of the compliance at the wrist joint is verified with the help of human kinematic model.

The structure of the paper is as follows. The mechanical design is explained in section II, section III proposes kinematic model of human lower-arm, performance evaluation is presented in section IV and conclusion appears in section V.

## II. Mechanical Design

The mechanical design of the 6 DoF exoskeleton robot [see Fig. 1] is presented in this section. The design consists of 4 units to generate elbow flexion-extension, forearm supination-pronation, wrist ulnar-radial deviation and wrist flexion-extension. Four active DoF are used to obtain the motions and 2 passive DoF are included at elbow and wrist by means of the flexible bellow couplings.

### *A. Elbow motion unit*

The elbow flexion-extension is generated with respect to the link which connects to fixed frame. Rear end of the link connected to fixed frame [see Fig. 2(a)] is designed to attach the robot to the wheel chair through a shoulder exoskeleton with passive mechanism. Since most of the physically weak people use wheel chair this configuration allows them to perform daily activities.

One bellow coupling is connected at elbow joint and its two hubs are connected between distal link and fixed frame [see Fig. 2(b)]. This connection allows passive compliance of bellow coupling along the elbow axis.

The drive motor (Maximum torque 8.3 Nm) of the elbow joint is attached to the distal link of forearm [see Fig. 2(a)]. Motor shaft is directly coupled to the distal end of the flexible bellow coupling by means of set screws. Since distal end of the bellow coupling is press fitted with distal link, oscillatory motion of the motor generates elbow flexion-extension.

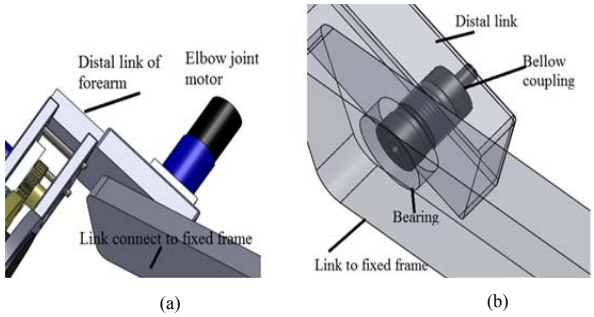


Figure. 2. Flexible bellow coupling at elbow joint

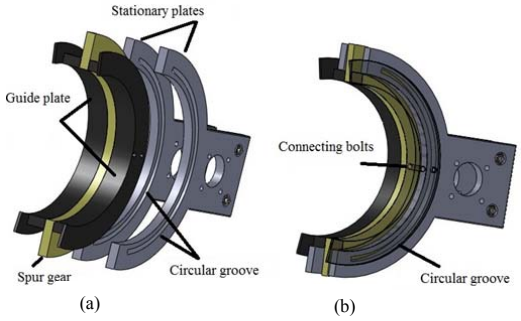


Figure. 3. Forearm motion unit: (a) disassemble view, (b) assemble view

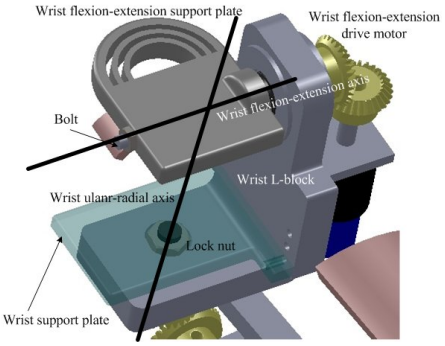


Figure. 4. Wrist motion axes of the exoskeleton robot

### *B. Forearm motion unit*

In order to reduce the overall weight of the exoskeleton, an open arm structure is designed to generate the forearm motion. Two stationary plates are used to hold the moving parts of the forearm motion unit [see Fig. 3(a)]. Further, the moving part consists of two guide plates and semi-circular spur gear [see Fig. 3(a)]. Moreover, the motion of forearm unit is supported with sliding action between guide plate and stationary plate along the semi-circular groove of the stationary plate [see Fig. 3(b)].

Forearm drive motor (Maximum torque 3.3 Nm) is fixed to the stationary plates of the forearm motion unit [see Fig. 1]. Spur pinion is attached to the motor shaft which drives the semi-circular spur gear. Two guide plates which are surrounded by semi-circular spur gear [see Fig. 3(a)], move along the groove of the stationary plates. This oscillatory motion generates the forearm supination-pronation.

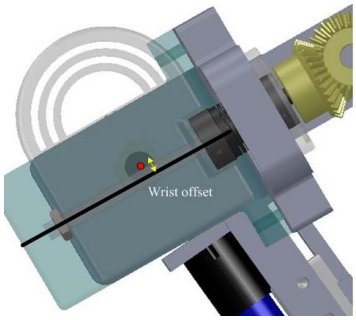


Figure. 5. Axis offset at the wrist motion unit

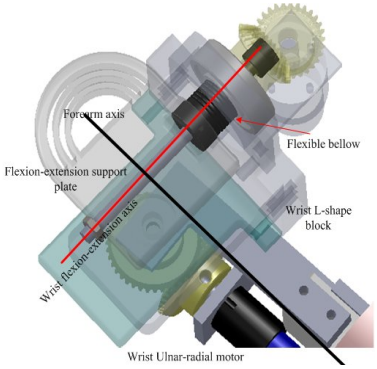


Figure. 6. Wrist flexion-extension with flexible bellow coupling

### C. *Wrist motion unit*

Typically, human wrist has a complex anatomical structure. Two DoF motions, flexion-extension and ulnar- radial deviation are generated in the wrist. According to the wrist anatomy, flexion-extension axis and ulnar-radial axis do not passes through a same point in the wrist and there exists an offset between two rotational axes [11]. Further, the amount of offset is a subject depended parameter [12]. Therefore, wrist L-shape block of the exoskeleton robot is designed to accommodate wrist flexion-extension axis and wrist ulnar-radial deviation axis [see Fig. 4]. Moreover, two wrist axes are placed with 5 mm offset from each other [see Fig. 5]. Further, to provide comfortable feeling to the wearer, wrist support plate [see Fig. 4] is designed to alter the position along ulnar-radial deviation axis in order to accommodate different sizes of human wrist. The details of wrist flexion-extension and ulnar-radial deviation are presented in the following subsections.

*Wrist flexion extension unit*

Wrist flexion-extension is supported with a flexible bellow coupling. One end of the bellow is connected to the drive motor (Maximum torque 1.8 Nm) side and other end is connected to wrist flexion- extension support plate through a bolt [see Fig. 4]. Therefore, oscillatory motion of the motor generates wrist flexion-extension. Moreover, Velcro straps are used to hold the wearer wrist on flexion-extension support plate. Since, wrist flexion-extension generates around two different axes [13], the compliance at wrist joint by means of flexible bellow coupling causes to provide comfortable feeling

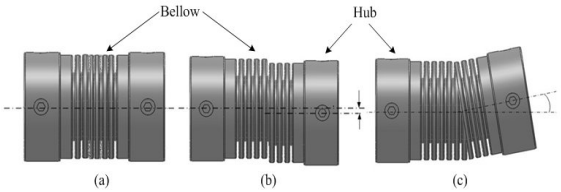


Figure. 7. Types of misalignments in flexible bellow coupling (a) axial (b) parallel (c) angular

to wearer when performing daily activities. This aspect promotes the pHRI in the exoskeleton robot.

*Wrist ulnar- radial deviation unit*

Ulnar-radial deviation is generated at base of the L-shape wrist block. Further, the ulnar-radial drive motor (Maximum torque 1.8 Nm) is attached to base of the wrist L-block [see Fig. 6]. A bevel gear pair is used to generate ulnar- radial deviation of the exoskeleton robot. The driven bevel gear shaft is connected to wrist L-block through a lock nut [see Fig 4]. Therefore, oscillatory motion of the motor is transmitted to wrist L-block which generates the ulnar-radial deviation.

*Flexible Bellow Coupling*

The bellow coupling in [14] is used to obtain the compliance in the 6 DoF exoskeleton robot. This bellow coupling is an advancement of flexure and it has three type of misalignments: axial, parallel and angular [see Fig. 7]. This feature is an attractive solution to exoskeleton robot in order to avoid joint axes misalignment between human and robot. Other than the compliance in bellow coupling, the motion in translational direction contributes as the passive DoF. Therefore, the bellow coupling gives compliance as well as passive DoF to the exoskeleton robot. Further, the added DoF causes to modify the Jacobian (by increasing number of columns) of the robot and alter the kinematic performance.

The bellow coupling mainly consists of hub and bellow [see Fig. 7]. The hub at both ends used to connect the shaft to the bellow coupling by means of set screws. The middle section consists of flexible bellow made from Phosphor Bronze. This coupling has low weight (0.016 kg), low inertia ($9.9 \times 10^{-7}$ kgm$^2$), high stiffness (180 Nm/rad) and zero backlash. Further, those features are desirable to obtain high quality interface in pHRI in exoskeleton robots [1].

Two bellow couplings are used in the 6 DoF upper limb exoskeleton robot. One coupling is connected at the elbow joint and the other is connected at the wrist joint. Further, joint axes misalignment between human and robot are significant at elbow and wrist joint due to presence of anatomical complexity [4][11]. Therefore, compliance of the bellow coupling minimizes the effect due joint axes misalignment between human and robot. Other than the above reason, position of bellow coupling contributes kinematic redundancy of serial manipulators. According to [15], redundancy in a serial link manipulator can be achieved by proper placement of joints and in case of the 6 DoF exoskeleton, positioning two prismatic joints with parallel axes [see Fig. 1] causes for the redundancy.

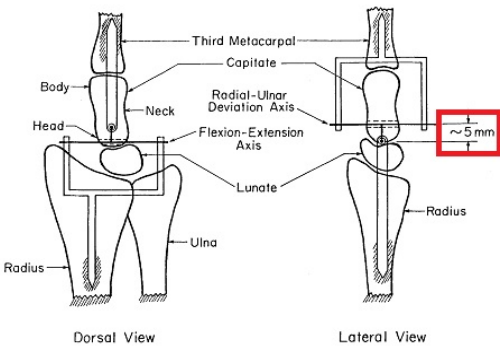


Figure. 8. Wrist axis offset [11]

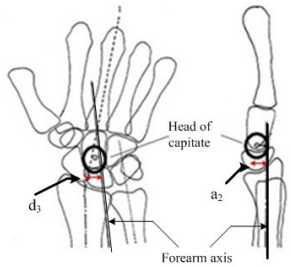


Figure 9. Position of head of capitate with respect to forearm axis [11]. $a_2$ is deviation of head of capitate from forearm plane. $d_3$ is deviation of head of capitate from forearm axis towards radial direction

## III. Kinematic Model of Human Lower Arm

Since upper limb exoskeleton robots are closely interact with human limb, understanding of human kinematic cannot be neglected in relation with the design of exoskeleton robots. However, due to the presence of complexity of human anatomy, it is difficult to identify the exact position of axes, centre of rotation, displacements in human bones due to the presence of soft tissues, muscles in the human body. However, taking complexity of upper limb, different models are proposed in the literature with several DoF. In [3], 9 DoF kinematic model is proposed for upper limb and 4 DoF is used to define the kinematics in lower arm. A 7 DoF model is proposed in [16] and human lower arm is defined with 4 DoF. Further, a 4 DoF kinematic model is proposed for human lower arm in [17]. In many instances kinematic of human lower arm is modeled with 4 DoF. This includes one DoF at elbow, and three DoF at wrist. However, human wrist has a complex anatomical structure and it consists of different bones, such as carpal and metacarpals. The wrist flexion-extension axis is located at head of capitate, which is one of the carpal bone in human wrist. The axis of wrist ulnar-radial deviation is not passes through a head of capitate and it has a offset of 5 mm from flexion-extension axis [11]. Fig. 8 shows the position of wrist axes with respect to head of capitate at wrist joint. Typically, wrist axis offset is taken as 8 mm for majority of subjects [12]. Taking those facts into account, kinematic model for human lower arm is proposed in this study. Further, it was realized that head of capitate is not coincident with forearm axis [11]. It has a offset toward radial side (for right hand) and further it deviates from plane which passes through a forearm axis [11]. Fig. 9 shows the deviation of head of capitate with respect to forearm axis for right hand.

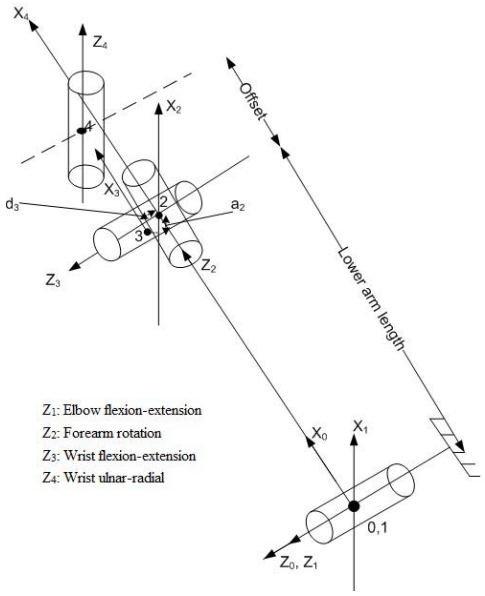


Figure 10. Proposed 4 DoF kinematic model for human lower arm

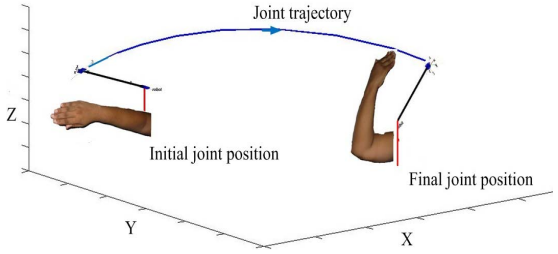


Figure 11. Joint trajectory for 6 DoF exoskeleton robot defined in Matlab.)

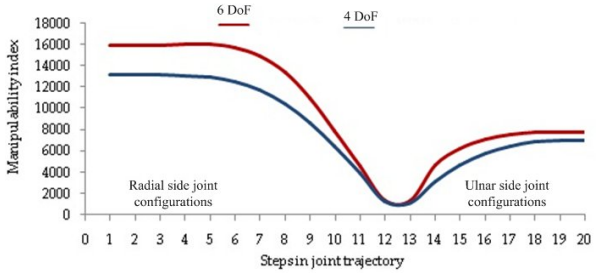


Figure 12. Comparison of manipulability index with/without the flexible bellow coupling

Considering those factors, 4 DoF kinematic model is improved and shown in Fig 10. Typically, the value of $d_3$ and $a_2$ mentioned in human kinematic model is not constant and vary with subjects. The measure of $a_2$ depends on length of third metacarpal bone while, $d_3$ depends on width of ulnar-radial axis of human lower arm [18].

## IV. Performance Evaluation

Different measures can be used to evaluate performance of pHRI in exoskeleton robot. Moreover, ease on manipulation of exoskeleton robot is an important measure to evaluate dexterity of the robot. Therefore, degree of manipulation of

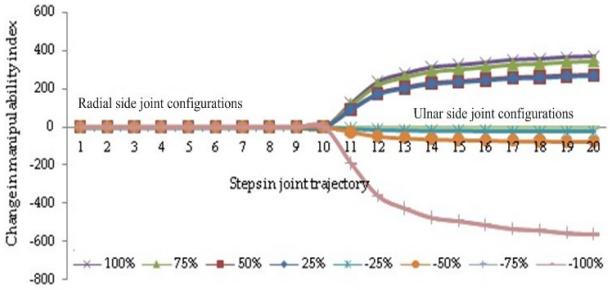


Figure 13.Variation of manipulability index against different $a_2$

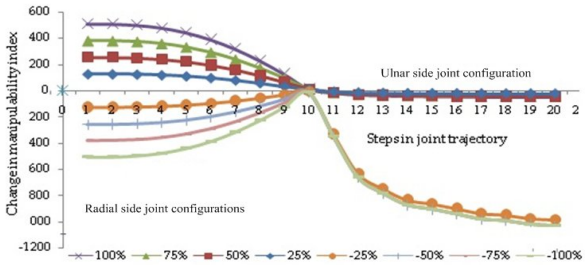


Figure 14. Variation of manipulability index against different $d_3$

the 6 DoF robot is evaluated based on Manipulability index [19]. Joint trajectory for the 6 DoF robot is defined in between two extreme joint configurations [see Fig. 11], using Matlab/Robotic toolbox [20] and divided it into 20 equal steps and manipulability index is evaluated at each step based on (1), where $J$ is robot Jacobian and $W(J)$ is a manipulability index.

$$W(J) = \sqrt{\det(J.J^T)} \quad (1)$$

In order to evaluate variation of manipulation due to effect of redundancy from the bellow coupling, manipulability index is re-evaluated with absence of two passive DoF. The comparison of variation of manipulability index is shown in Fig. 12. Further, readers are encouraged to refer [21] for more details of redundancy in the 6 DoF exoskeleton robot.

According to the result shown in Fig. 12, the dexterity of 6 DoF exoskeleton robot to perform daily activities is improved since the availability of passive DoF through the flexible bellow coupling. The analysis results show that redundancy causes to improve the maximum manipulability by 21.13 %, while minimum manipulability also improved by 22.25 %.

### A. *Sensitivity analysis of manipulability measure for human kinematic model*

Joint trajectory for human model is defined in between two joint configurations (initial pose and final pose) and manipulability index is evaluated for each joint step and repeated for all joint steps. During manipulability evaluation, average values are taken for the links: 250 mm for lower arm length and 8 mm for wrist axes offset. $a_2$ is taken as 0.646 mm and $d_3$ is taken as 1.5 mm. However, intra-subject variations of wrist parameters, such as $a_2$ and $d_3$ are more dominant than variations of other parameters [18]. Therefore, in order to identify the effect of variations of manipulability index due to

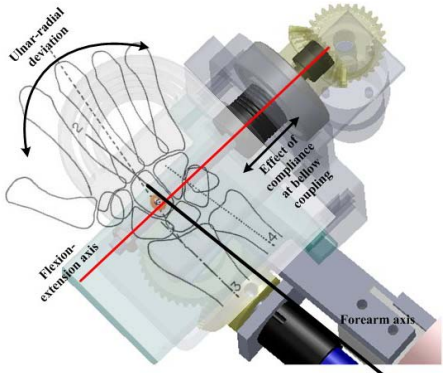


Figure 15. Passive compliance at wrist joint due to the flexible bellow coupling

$a_2$ and $d_3$: their values are changed by 25% [see Table 1] within allowable range and manipulability index is determined at each value. The variation of manipulability index for each percentage of $a_2$ and $d_3$ are shown in Fig. 13 and Fig. 14 respectively. Since 6 DoF exoskeleton is designed to wear in human right hand, manipulation in radial side of the joint trajectory is more important than that of ulnar side of the joint trajectory. According to the Fig. 13 and 14, variation of $a_2$ has an effect to alter the manipulability index in ulnar side of the joint trajectory. Nevertheless, manipulability in radial side is more sensitive to the variation of $d_3$. Further, this analysis shows that increasing the value of $d_3$ causes to improve the manipulability index of human lower arm model.

### B. *Passive compliance in the 6DoF exoskeleton robot*

The variation of manipulability index in human kinematic model with respect to $d_3$ is an interesting result and this aspect is taken into design the 6 DoF exoskeleton robot. Analysis shows that, higher $d_3$ causes to improve the manipulability index. Therefore, passive compliance of the flexible bellow coupling contributes wrist ulnar-radial deviation due to positioning it in wrist flexion-extension axis. Moreover, compliance facilitates the motion in wrist flexion-extension direction due to presence of the passive DoF. Therefore, exoskeleton robot facilitates smoother wrist motion due to improvement in positioning the head of capitate towards radial direction from forearm axis. This effect is illustrated in Fig. 15. Double head straight arrow shows the motion of flexible bellow coupling due to passive DoF under compliance.

TABLE 1. VARIATIONS OF PERCENTAGES AND VALUES FOR $a_2$ AND $d_3$

| PERCENTAGE % | $a_2$ (mm) | $d_3$ (mm) |
|---|---|---|
| 100(upper limit) | 0.699 | 1.75 |
| 75 | 0.686 | 1.687 |
| 50 | 0.673 | 1.625 |
| 25 | 0.659 | 1.563 |
| 0 (average) | 0.646 | 1.5 |
| -25 | 0.632 | 1.437 |
| -50 | 0.619 | 1.375 |
| -75 | 0.606 | 1.312 |
| -100 (lower limit) | 0.592 | 1.5 |

Double head curve arrow shows the ulnar-radial deviation. Therefore, when wearer performs ulnar-radial deviation, the presence of passive DoF with compliance in the flexible bellow coupling enhances the distance $d_3$. Further, axis misalignments of the flexible bellow coupling in angular and parallel directions causes to minimizes the kinematic discrepancies due to joint axes variation of human and robot, specially at wrist and elbow.

## V. Conclusion

This paper proposed a design of upper limb exoskeleton taking passive DoF with compliance. The compliance was introduced to the exoskeleton robot by means of a flexible bellow coupling. Those couplings were connected in order to improve kinematic redundancy. The variation of manipulability index with respect to flexible bellow coupling was analyzed to identify redundancy in the robot kinematic chain. Results revealed that, redundancy improves the manipulability index by 21.13%. Kinematic model of human lower arm was presented considering wrist axes offset and variation of head of capitate of human wrist. Sensitivity of hand manipulability index was determined against to wrist parameters and significance of presence of passive compliance at wrist joint was identified with respect to kinematic model of human lower arm. Moreover, simulation of joint trajectory was presented to verify the improvement in dexterity due to embedding redundancy via flexible bellow coupling.

## Acknowledgment

The Authors would like to acknowledge the support given by National Research Council of Sri Lanka (grant no. 11-067).

## References

[1] A. Gupta, and M. K. O. Malley, "Design of a Haptic Arm Exoskeleton for Training and Rehabilitation," *IEEE/ASME Transactions on Mechatronics*, vol. 11, no. 3, pp. 280–289, 2006.

[2] J. L. Pons, Ed., *Wearable Robots*. John Wiley & Sons, Ltd, 2008.

[3] A. Schiele, "Fundamentals of Ergonomic Exoskeleton Robots," *Ph.D Dissertation*, Delft University, 2008.

[4] M. Esmaeili, K. Gamage, E. Tan, and D. Campolo, "Ergonomic Considerations for Anthropomorphic Wrist Exoskeletons: A Simulation Study on the Effects of Joint Misalignment," in *Proc. of IEEE/RSJ International Conference on Intelligent Robots and Systems*, 2011, pp. 4905–4910.

[5] M. Cempini, S. Marco, M. De Rossi, T. Lenzi, N. Vitiello, and M. C. Carrozza, "Self-Alignment Mechanisms for Assistive Wearable Robots : a Kineto-Static Compatibility Method," *Proc. of IEEE Transactions on Robotics*, vol. 29, no. 1, pp. 236-250, 2013.

[6] M. Mihelj, "Human Arm Kinematics for Robot Based Rehabilitation," *Robotica*, vol. 24, no. 03, pp. 377–383, 2006.

[7] J. Yang, K. A. Malek, and K. Nebel, "Reach Envelop of A 9-Degree of Freedom Model of The Upper Extremity," *International Journal of Robotics and Automation*, vol. 20, no. 4, pp. 240–259, 2005.

[8] M. F. Chan, D. R. Giddings, C. S. Chandler, C. Crags, R. D. Plant, and M. C. Day, "An Experimentally Confirmed Statistical Model on Arm Movement," *Human Movement Science*, vol. 22, no. 02, pp. 631–648, 2004.

[9] J. C. Perry, J. Rosen, and S. Burns, "Upper-Limb Powered Exoskeleton Design," *IEEE/ASME Transactions on Mechatronics*, vol. 12, no. 4, pp. 408–417, 2007.

[10] W. Yu and J. Rosen, "A Novel Linear PID Controller for an Upper Limb Exoskeleton," in *Proc. of IEEE Conference on Decision and Control*, 2010, pp. 3548–3553.

[11] Y. Youm and A. Flatt, "Design of a Total Wrist Prosthesis," *Annals of Biomedical Engineering*, vol. 12, pp. 247–262, 1984.

[12] L. Leonard, D. Sirkett, G. Mullineux, G. Giddins, and A. Miles, "Development of an In-Vivo method of Wrist Joint Motion Analysis," *Journal of Clinical Biomechanics*, vol. 20, no. 2, pp. 166–171, 2005.

[13] D. Thompson, "Wrist Joint Complex," 2011. [Online]. Available: www.moon.ouhsc.edu/dthompso/namics/wrist.htm#move. [Accessed: 27-Jan-2014].

[14] SDP-SI, "Set screw type hub bellow coupling," 2013. [Online]. Available: https://sdp-si.com/estore/catalog/group/1057. [Accessed: 12-May-2013].

[15] W. Khalil and E. Dombre, *Modeling, Identification and Control of Robots*, 1st ed. Kogan Page Science, 2004.

[16] J. Rosen, J. C. Perry, N. Manning, S. Burns, and B. Hannaford, "The Human Arm Kinematics and Dynamics During Daily Activities – Toward a 7 DoF Upper Limb Powered Exoskeleton," in *Proc. of* 12th *International Conference on Advanced Robotics- ICAR*, 2005, pp. 24–32.

[17] M. K. O. Malley, A. Gupta, V. Patoglu, and C. Burgar, "Design , Control and Performance of RiceWrist: A Force Feedback Wrist Exoskeleton for Rehabilitation and Training," *International Journal of Robotics Research*, vol. 27, no. 2, pp. 233–251, 2008.

[18] A. Buryanov and V. Kotiuk, "Proportions of Hand Segments," *International Journal of Morphol*, vol. 28, no. 3, pp. 755–758, 2010.

[19] T. Yoshikawa, "Manipulability of Robotic Mechanisms," The *International Journal of Robotic Research*, vol. 4, no. 3, pp. 2–9, 1985.

[20] P. I. Corke, "A robotic toolbox for MATLAB," *IEEE Robotics and Automation Magazine*, pp. 24–32, Sep-1996.

[21] J. M. P. Gunasekara, R. A. R. C. Gopura, T. S. S. Jayawardane, and G. K. I. Mann, "Dexterity Measure of Upper Limb Exoskeleton with Improved Redundancy," in *Proc. of IEEE International Conference on Industrial and Information Systems*, 2013, pp. 548–553.